Microphase Separation and Conductivity Behavior of Poly(propylene oxide)–Lithium Salt Electrolytes

C. Vachon, C. Labrèche, A. Vallée, S. Besner, M. Dumont, and J. Prud'homme*

Department of Chemistry, University of Montréal, Montréal, Québec, Canada H3C 3J7

Received April 7, 1995; Revised Manuscript Received May 25, 1995[⊗]

ABSTRACT: A DSC study performed on poly(propylene oxide) (PPO) electrolytes containing various lithium salts (LiBr, $LiClO_4$, $LiCF_3SO_3$, and $LiN(CF_3SO_2)_2$) shows that microphase separation is a general feature of PPO–LiX systems. Below a certain salt content, which corresponds to O/Li = 9 (O = ether oxygen) for LiBr, to O/Li = 10 for $LiClO_4$ and $LiCF_3SO_3$, and to O/Li = 16 for $LiN(CF_3SO_2)_2$, two glass transition (T_g) features are recorded on optically clear mixtures of these systems. A comparison made with poly(ethylene oxide) (PEO) electrolytes shows that this phase complication has a strong effect on the conduction process. For the PPO–LiBr and PPO–$LiClO_4$ systems, which involve a large difference between the compositions of their low-T_g and high-T_g microphases, a percolation threshold occurs over the range where related PEO–LiX electrolytes exhibit their conductivity maximum. A similar but less pronounced effect is systematically observed for the other PPO–LiX systems and for non-PPO systems that exhibit an initial accelerated rise in their T_g-composition relationships. The PEO–LiX systems are free from these anomalies.

Introduction

The broad range of potential applications of polyether–metal salt solid electrolytes, particularly as thin-film separators in lithium rechargeable batteries, has stimulated a large number of basic studies in recent years.[1,2] In their optimal form, these electrolytes are rubbery materials of low glass transition temperature (T_g) that involve liquidlike molecular motion at the microscopic level. In this form, they show great similarity with the aprotic, liquid electrolytes currently used in primary batteries.[3] Their conductivity exhibits a broad maximum in the concentrated regime and, for a given concentration over this range, decreases exponentially with decreasing temperature toward T_g. A marked difference, however, lies in the diffusion mechanism of the solvated ions. Since metal ions (particularly Li^+) strongly coordinate to the polymer units, they undergo long-range migration through an exchange of solvation sites instead of moving with their solvation spheres. This feature, together with the strong ion–ion interactions resulting from the low permittivity of polyethers,[4,5] is detrimental to metal cation transport in direct current devices based on polyether electrolytes. To clarify the physics underlying these effects, rubbery and liquid electrolytes prepared with commercial or laboratory-made polyethers are currently investigated by various physical and electrochemical techniques.

Poly(ethylene oxide) (PEO), which is a linear analog of crown ethers, is probably the best solvating polyether for a number of metal salts. However, this polymer, which is prone to crystallize, forms crystalline compounds with most of these salts. For that reason, special care must always be taken to define the liquidus curves of these compounds prior to physical studies on PEO melted or supercooled electrolytes.[4,5] In order to avoid this difficulty, several basic studies, particularly on ion association,[6–13] were recently conducted on noncrystallizable electrolytes prepared with low molecular weight atactic poly(propylene oxide) (PPO). Unfortunately, as previously shown on mixtures of $LiClO_4$, $NaClO_4$, and NaI prepared with such a polymer, a more insidious phase effect arises because PPO has a lower solvating power than PEO.[14]

Below a certain salt content, which corresponds to a molar ratio O/salt = 10 (O = ether oxygen) for the PPO–$LiClO_4$ and PPO–NaI systems and to a molar ratio O/salt = 13 for the PPO–$NaClO_4$ system, a liquid–liquid separation takes place. For the former two systems, this separation is microscopic. The mixtures are optically clear but exhibit two T_g features in their DSC curves. According to a quantitative analysis of these curves, more dilute mixtures of these systems essentially consist of complexed microdomains with a 10/1 (O/salt) stoichiometry in equilibrium with salt-free PPO. This microscopic separation is a genuine phase feature since the mixtures of the third system (PPO–$NaClO_4$) exhibit a two-layer separation at room temperature. Upon heating above 40–50 °C, however, their macroscopic separation reversibly transforms into a microscopic separation.

Although the high-T_g feature in the DSC curves of these systems progressively broadened with dilution to disappear for O/salt > 20, complementary information on more dilute mixtures could be deduced from independent data. These data were Raman spectra previously reported by Schantz and Torell[6,7] for mixtures of $LiClO_4$ (and $NaCF_3SO_3$) with a PPO sample of the same molecular weight ($M = 4 \times 10^3$) as in our study. In this work dealing with ion association, spectra had been recorded at 22 °C over a wide range of compositions (5 < O/salt < 1000) by focusing on the anion symmetric stretching mode. Upon dilution from O/salt = 5, the components of a band splitting assigned to ion pairs and free anions exhibited a marked change in relative intensities down to O/salt = 10 (O/salt = 16 for $NaCF_3SO_3$). For salt contents below this limit, however, the band splitting remained finite with essentially no further change in relative intensities down to O/salt = 1000. Not only was this feature consistent with our interpretation, but it also revealed that $LiClO_4$ (or $NaCF_3SO_3$) was confined to local regions of invariant stoichiometry over a wide range of concentrations in the dilute regime.

Since the Raman features of the PPO–$NaCF_3SO_3$ system are similar to those of the PPO–$LiClO_4$ system,

[⊗] Abstract published in *Advance ACS Abstracts,* July 1, 1995.

0024-9297/95/2228-5585$09.00/0

we concluded that a microphase separation also takes place in the mixtures of this system.[14] Interestingly, this feature has recently been confirmed by Bergman *et al.*[15] on the basis of a photon correlation relaxation study. Like the DSC technique, this light scattering technique yielded evidence for two relaxation processes over a limited range of compositions only. As proposed in the former work,[14] this suggests that the size of the complexed microdomains decreases markedly with decreasing global salt content. They probably transform into more and more labile heterogeneities that eventually fluctuate at a rate high enough to become undiscernible from the bulk relaxation of the materials. In Raman spectroscopy, however, these heterogeneities appear as static down to high dilution (O/salt = 1000).

Over 25 years ago, Moacanin and Cuddihy[16] had already reported thermomechanical data showing two relaxation features for PPO–$LiClO_4$ mixtures prepared with a high molecular weight PPO. More recently, Greenbaum *et al.*[17] had also reported DSC data showing two T_g features for PPO–NaI and PPO–NaSCN mixtures prepared with a similar polymer. In both these studies, the PPO samples were commercial rubbers containing a small fraction of allyl glycidyl ether units to permit sulfur vulcanization. Since our work, Nekoomanesh *et al.*[18] reported a T_g splitting for mixtures of $LiClO_4$ with high molecular weight propylene oxide–ethylene oxide statistical copolymers with EO molar contents in the range 64–90%. From these studies, it is clear that the liquid–liquid separation in the $M = 4 \times 10^3$ low molecular weight PPO did not result from its finite content (3 mol %) in hydroxy end groups.

This separation, which is not observed for supercooled mixtures of $LiClO_4$ or NaI with PEO,[14] probably results from an unfavorable balance between the cation–oxygen interactions, which favor salt dispersion, and the ion–ion long-range Coulombic interactions, which oppose this dispersion. A biphasic liquid–liquid structure becomes more stable than a homogeneous structure because the dominant factor is the Coulombic energy liberated through the ion condensation process associated with the formation of the high-T_g microphase. As pointed out in the former work, evidence for a more discrete separation can be found in the T_g–composition relationships previously reported for noncrystallizable mixtures of MSCN (M = Li, Na, and K) with atactic poly(methyl glycidyl ether) (PMGE).[19] For this polyether, which has a solvating power intermediate between PEO and PPO, an accelerated rise in T_g occurs over the same range of compositions as the T_g splitting related to PPO. Note that such an accelerated rise in T_g was also observed for supercooled mixtures of the PEO–$NaClO_4$ system.[14] All these anomalies, particularly those in PPO, call for a more systematic investigation.

In the first part of this paper, we report DSC data obtained for three other PPO–lithium salt systems. From these data, which concern mixtures of LiBr, $LiCF_3SO_3$, and $LiN(CF_3SO_2)_2$ with a $M = 4 \times 10^3$ PPO, it turns out that microphase separation is a general feature of PPO–LiX electrolytes. However, a comparison based on the derivatives of the DSC curves shows that the compositions of both the low- and high-T_g microphases depend on the nature of the anion. The smallest difference between these compositions is observed for the PPO–$LiN(CF_3SO_2)_2$ system, while the largest difference is observed for the PPO–$LiClO_4$ system. Therefore, these two salts, which exhibit comparable, high conductivities in PEO,[20] are well suited for examining the effect of microphase separation on the conductivity of PPO electrolytes.

Since conductivity data already exist in the literature for the PPO–$LiClO_4$ and PPO–$LiCF_3SO_3$ systems,[8,9] measurements were made on the PPO–LiBr and PPO–$LiN(CF_3SO_2)_2$ systems only. The investigation of these four systems, presented in the second section of this paper, is based on a comparison with related PEO amorphous electrolytes of the same compositions. In the case of LiBr, an oxymethylene-linked PEO was used because this salt forms a crystalline compound of high melting point (332 °C) with regular PEO. This sample, denoted as P(OM/PEG200), was a high molecular weight, noncrystallizable material prepared from a poly(ethylene glycol) oligomer (PEG200). This investigation, which also includes a comparison between the PMGE–LiSCN and PEO–LiSCN systems, reveals the presence of a systematic effect, reminiscent of a percolation threshold, for all the systems that exhibit DSC evidence for a microscopic liquid–liquid separation.

Experimental Section

Materials. PEO ($M_n = 4.4 \times 10^3$, $M_w/M_n = 1.02$) and PPO ($M_n = 4.2 \times 10^3$, $M_w/M_n = 1.35$) were the same as those used in the former work.[14] P(OM/PEG200) ($M_n = 5.3 \times 10^4$, $M_w/M_n = 2.5$) was prepared according to the procedure described by Booth *et al.*,[21] by reacting a PEG200 oligomer ($M_n = 223$, $M_w/M_n = 1.04$) with an excess of dichloromethane in the presence of KOH. PMGE ($M_n = 2.5 \times 10^4$, $M_w/M_n = 1.8$) was prepared by anionic polymerization by using potassium *tert*-butoxide as the initiator and tetrahydrofuran as the solvent. The details concerning synthesis, purification, and characterization of these two polymers are reported in previous papers.[4,19] Before utilization, all the polymers were dried under high vacuum for 48 h. Their residual conductivities at 100 °C were lower than 5×10^{-8} S/cm.

$LiClO_4$ (K&K, 99.8%) and $LiCF_3SO_3$ (Aldrich, 97%) were dried under high vacuum for 24 h at 130 °C. LiBr (MCB, 99%) and $LiN(CF_3SO_2)_2$ (3M), which exhibited dehydration endotherms at 168 and 166 °C, respectively, were dried under high vacuum for 24 h at 150 °C and for an additional 1 h at 170 °C. Polymer–salt mixtures were prepared under a dry atmosphere by mixing weighed quantities of 1–5% methanol solutions of each component. Solvent evaporation was carried out in ampules connected to a vacuum system. The solvent-free mixtures were transferred into 25-mm-diameter, optically clear, glass vials with screw caps and dried under high vacuum for 24 h at 130 °C. Those containing LiBr and $LiN(CF_3SO_2)_2$ were dried for an additional 1 h at 170 °C. The vials were stored under a dry atmosphere in a glovebox.

DSC Measurements. The calorimeter (Perkin-Elmer DSC-4) was flushed with dry helium, and sample pans were filled and sealed under a dry atmosphere in the glovebox. Glass transition features were recorded at a heating rate of 40 °C/min, and supercooled specimens (with PEO) were obtained by melt quenching at a cooling rate of 320 °C/min. Values of T_g were read at the intersection of the tangent drawn through the heat capacity jump, with the base line recorded before the transition. Heat capacity increases, Δc_p, at T_g were read at the temperature corresponding to the half-height of the transitions. In the case of the PEO–LiBr system, fusion and dissolution temperatures were read at the peak of the endotherms. PEO (or eutectic) melting was recorded at 10 °C/min, while intermediate compound dissolution (or melting) was recorded at 40 °C/min. Although the mixtures of this system exhibited discoloration when heated above 250 °C under the microscope, an exothermic effect due to thermal degradation was noted above 350 °C only. All the high-temperature endotherms, even those at 332 °C, were well separated from this effect.

Conductivity Measurements. The bulk electrolytes were contained in cells consisting of two stainless steel solid

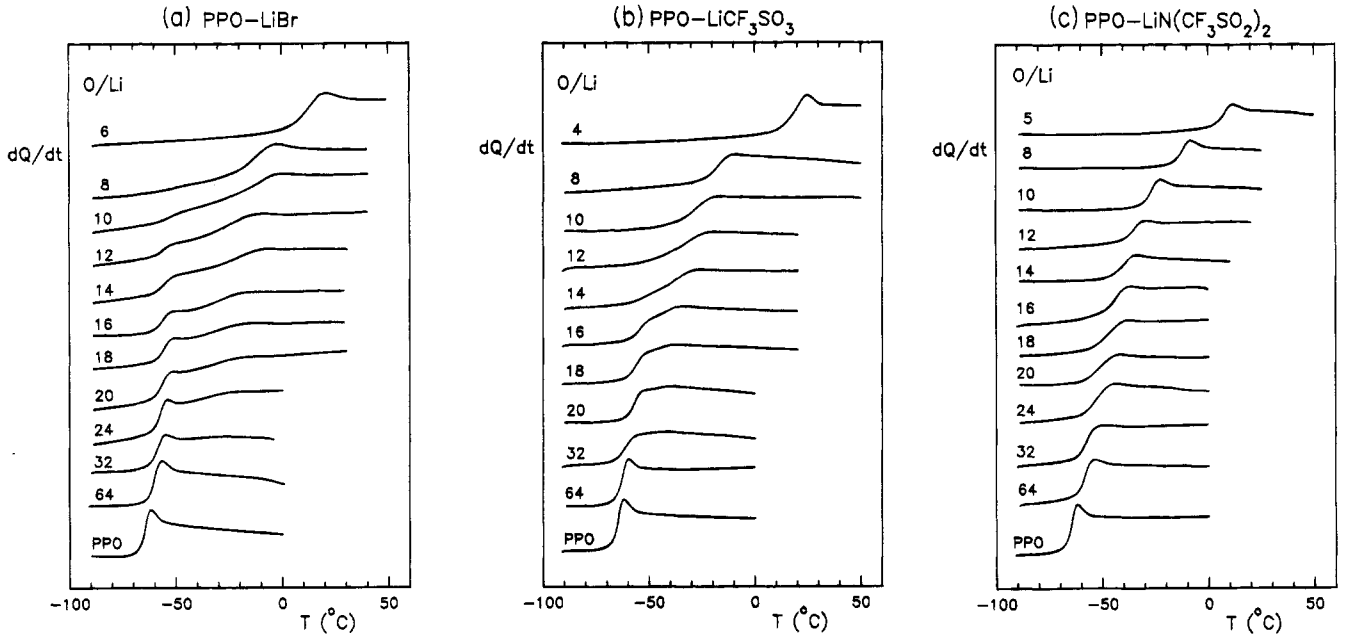

Figure 1. DSC heating curves recorded at 40 °C/min on mixtures of the PPO–LiBr (a), PPO–$LiCF_3SO_3$ (b), and PPO–$LiN(CF_3SO_2)_2$ (c) systems.

cylinders encapsulated at both ends of a Teflon ring. The cell assembly is fully described in a previous work.[5] A 1-cm-diameter disk-shape electrode–electrolyte contact surface was imposed by Teflon sleeves. The gap between the electrodes (3 mm) was measured at room temperature with an accuracy better than 1%, and no correction was made for the thermal expansion of the cells. The cells were filled and sealed in the glovebox. For that purpose, the bulk electrolytes were heated to 110–130 °C.

The conductivity measurements were performed in a Instron temperature chamber equipped with a computer-driven controller. The temperature of the electrolytes was measured with an accuracy better than ±0.2 °C by means of a thermocouple inserted in a well dug in the body of the cells. The real part, Z', and the imaginary part, Z'', of the complex impedance of the cells were measured over the frequency range 5 Hz to 13 MHz by using a Model 4192A Hewlett-Packard impedance analyzer. The impedance data were collected at intervals of 5 °C by means of a HP–IB interface. As usual,[5] the bulk dc resistance of the electrolyte was determined as the point where the high-frequency semicircle in the plot of Z'' as a function of Z' cuts the Z' axis.

Results and Discussion

(a) Thermal Properties. Figure 1 shows DSC curves recorded for various compositions of optically clear mixtures of PPO with LiBr, $LiCF_3SO_3$, and $LiN(CF_3SO_2)_2$. The curves related to LiBr are similar to those reported for $LiClO_4$ and NaI. They exhibit well-separated, double-T_g features over a range of compositions (10 < O/Li < 20). A T_g splitting is also observed for the PPO–$LiCF_3SO_3$ system. However, it is of lower magnitude and concerns a narrower range of compositions (14 < O/Li < 20). No T_g splitting is apparent for the PPO–$LiN(CF_3SO_2)_2$ system, but its single-T_g feature exhibit an abnormal broadening over the same range of compositions as the double-T_g features of the other systems.

Although the DSC curves recorded for the PPO–LiBr system are qualitatively similar to those reported for the PPO–$LiClO_4$ system, their quantitative analysis reveals some differences. The T_g data of these two systems are plotted as a function of the salt molar fraction in Figure 2. Near the critical composition for microphase separation (O/Li = 9 for LiBr and O/Li = 10 for $LiClO_4$), the low-temperature transition ($T_{g,L}$) associated with LiBr is higher than that associated with $LiClO_4$. In the former work on the PPO–$LiClO_4$ and PPO–NaI systems, the heat capacity increase (Δc_p, per gram of material) associated with $T_{g,L}$ was shown to increase linearly with decreasing salt weight fraction. Furthermore, in each case, the linear relationship extrapolated to the Δc_p value of PPO at a zero salt content. This feature, which is exemplified in Figure 3 for the PPO–$LiClO_4$ system, was interpreted as an indication that the low-T_g microphase related to this salt is essentially salt-free PPO. Included are the Δc_p data

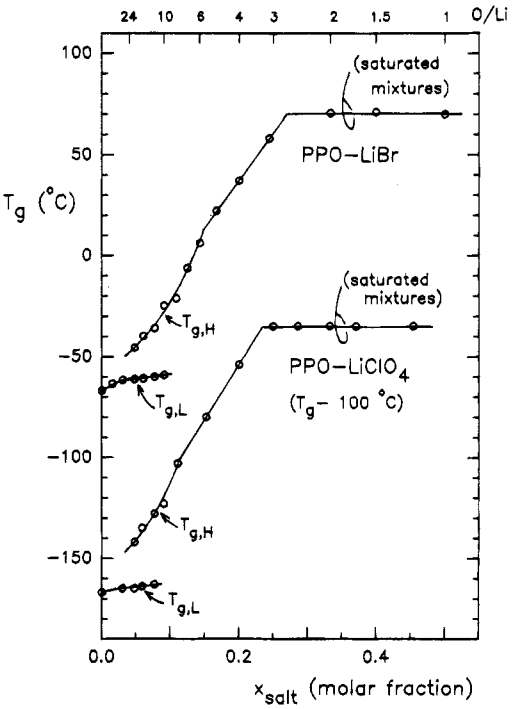

Figure 2. Plots of T_g as a function of the salt molar fraction for mixtures of the PPO–LiBr and PPO–$LiClO_4$ systems. $T_{g,L}$ and $T_{g,H}$ denote the onset of the low- and high-temperature features recorded below the critical composition for microphase separation (O/Li = 9 for LiBr, and O/Li = 10 for $LiClO_4$).

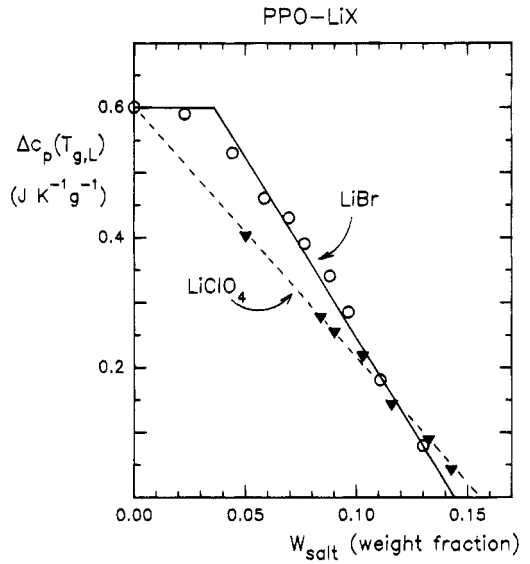

Figure 3. Plots of the heat capacity increase at $T_{g,L}$ (Δc_p, per gram of sample) as a function of the salt weight fraction for mixtures of the PPO–LiBr and PPO–$LiClO_4$ systems.

related to LiBr. In that case, the linear fit made over the range 10 < O/Li < 32, which intercepts the composition axis at $W_{salt} = 0.144$ (O/Li = 9), does not extrapolate to the value of salt-free PPO. The relationship exhibits a break at a finite salt content ($W_{salt} = 0.04$, O/Li = 40), suggesting the presence of a small amount of LiBr in the low-T_g microphase.

This interpretation in terms of an equilibrium between microphases of well-defined stoichiometries is not in contradiction with the fact that the onset of the high-temperature transition ($T_{g,H}$ in Figure 2) decreases markedly with decreasing global salt content. Nor is it in contradiction with the similar but less pronounced effect observed for $T_{g,L}$. Both these effects may be explained in terms of a change in the size of the microdomains with global dilution. Inspection of Figure 1 shows that the lowering of $T_{g,H}$ is associated with a marked, asymmetrical broadening of the high-temperature transition. By analogy with microphase-separated block copolymers,[22] this feature can be rationalized in terms of an exchange of kinetic energy through the chemical junctions at the interface between the unlike microphases.[14]

Over the range just below the critical composition, the biphasic structure related to LiBr (or $LiClO_4$) probably consists of dilute (or salt-free) microdomains dispersed into the more concentrated 9/1 (or 10/1) phase. In this situation, the segmental motion in the low-T_g microphase is expected to be dampened by the anchorage of some of its PPO segments to the continuous harder phase. It is likely that this effect accounts for a part of the small increase in $T_{g,L}$ with respect to salt-free POP. Such an effect was not observed for the PPO–$NaClO_4$ system, which exhibited a macroscopic separation over this range of compositions.[14] A further decrease in the global salt content has an effect comparable to a change in the relative chain length in a block copolymer. The size of the dilute microdomains increases to the detriment of the concentrated phase, and an inversion in the nature of the continuous phase takes place. At this point, a larger fraction of the polymer segments in the concentrated microphase are located near the interface where they undergo an exchange of kinetic energy with the more mobile phase. This surface effect, which increases with global dilution, probably accounts for both the asymmetrical broadening of $T_{g,H}$ and its fade-out at high dilution.

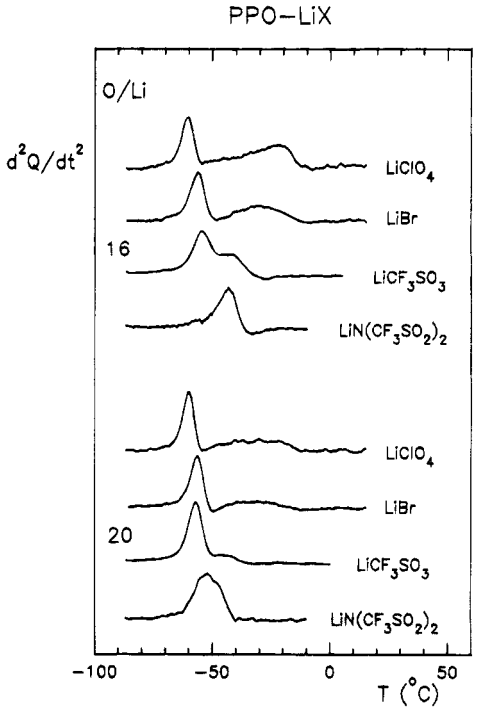

Figure 4. Comparison of the derivatives of the DSC curves recorded on O/Li = 16 and O/Li = 20 mixtures of the four PPO–LiX systems studied in this work.

Figure 4 shows the derivatives of the DSC curves of the O/Li = 16 and 20 mixtures of the four PPO–LiX systems. The peaks in these curves correspond to the points where the rate of change in heat capacity (dc_p/dt) due to each transition is maximum. They provide a better basis to examine the effect of the nature of the anions on $T_{g,L}$ and $T_{g,H}$. A more complete picture based on this procedure is given in Figure 5 for both the PPO–$LiCF_3SO_3$ and PPO–$LiN(CF_3SO_2)_2$ systems. It shows that the critical composition of the former system is located near O/Li = 10, like that of the PPO–$LiClO_4$ system. Furthermore, a shoulder indicating a T_g splitting is also apparent over the range 18 < O/Li < 24 for the PPO–$LiN(CF_3SO_2)_2$ system. At a given composition below the critical composition (O/Li = 16 for the latter system), the comparison made in Figure 4 shows that $T_{g,L}$ increases in the order $LiClO_4$ < LiBr < $LiCF_3SO_3$ < $LiN(CF_3SO_2)_2$, while $T_{g,H}$ decreases in the same order. The former feature suggests that the low-T_g microphases related to $LiCF_3SO_3$ and $LiN(CF_3SO_2)_2$ contain a larger amount of salt than that related to LiBr. Unfortunately, because of the proximity of $T_{g,L}$ and $T_{g,H}$, no reliable analysis based on Δc_p at $T_{g,L}$ can be made for these two systems. For the same reason, the plots shown in Figure 6, which summarize the T_g data of these two systems, are constructed on the basis of the onset of the first transition only.

According to a previous work on PEO–LiX electrolytes,[20] on a molar basis and over the range 6 < O/Li < 24, the T_g elevations produced by $LiCF_3SO_3$ and $LiN(CF_3SO_2)_2$ (2.9 and 2.8 °C/mol %, respectively) are markedly inferior to that produced by $LiClO_4$ (4.3 °C/mol %). Such data, which correspond to supercooled, homogeneous mixtures of these three salts with PEO, could not be obtained for the PEO–LiBr system. The phase diagram of this system (Figure 7) shows a high-temperature liquidus curve down to low concentrations (O/Li = 20).

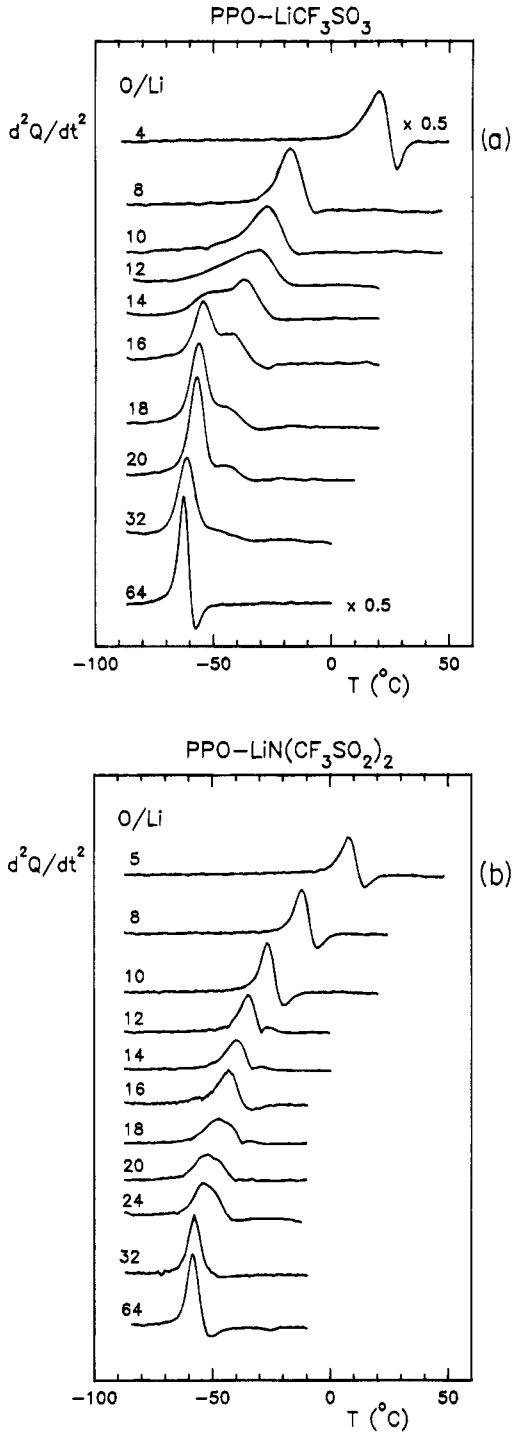

Figure 5. Derivatives of the DSC curves recorded on the mixtures on the PPO–$LiCF_3SO_3$ (a) and PPO–$LiN(CF_3SO_2)_2$ (b) systems. These derivatives allow a more accurate definition of the critical composition for microphase separation (O/Li = 10 for $LiCF_3SO_3$ and O/Li = 16 for $LiN(CF_3SO_2)_2$ than the DSC curves.

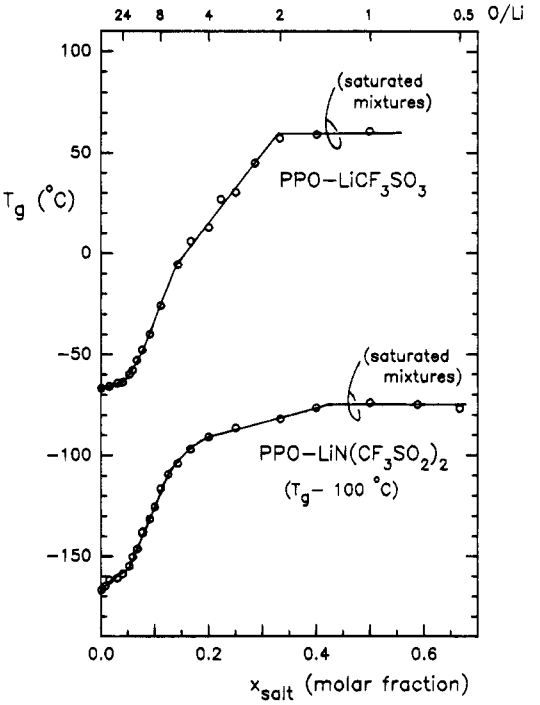

Figure 6. Plots of T_g as a function of the salt molar fraction for mixtures of the PPO–$LiCF_3SO_3$ and PPO–$LiN(CF_3SO_2)_2$ systems. Due to the overlapping of $T_{g,L}$ and $T_{g,H}$, these plots show the onset of the first transition only.

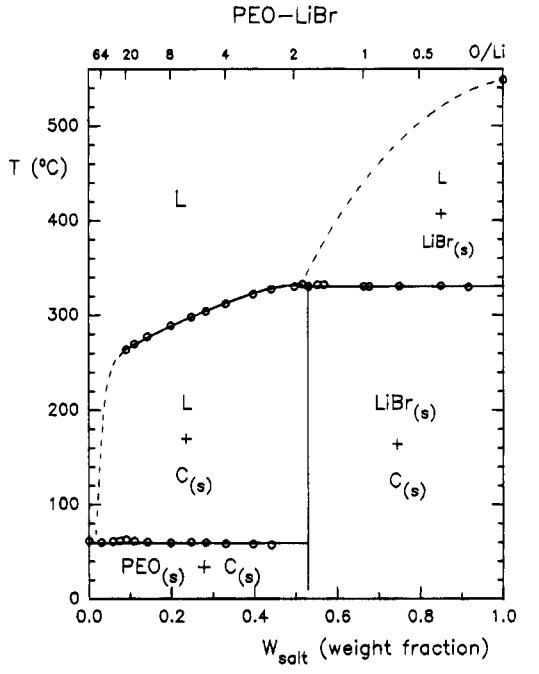

Figure 7. Phase diagram of the PEO–LiBr system. The vertical boundary at $W_{salt} = 0.53$ was derived from a calorimetric analysis of the DSC data. It shows the formation of a 1.75/1 (O/Li) crystalline compound that exhibits an incongruent melting at 332 °C. Mixtures with molar ratios O/Li = 1.85 and 1.60 had lower heats of fusion than the stoichiometric mixture.

For PPO, a reliable comparison of the T_g elevations produced by these four salts is possible at concentrations above the critical composition for microphase separation only. The T_g values of mixtures in a ratio O/Li = 6 with $LiClO_4$, $LiCF_3SO_3$, and $LiN(CF_3SO_2)_2$ are 16, −6, and −4 °C, respectively. They are systematically higher (by 23 ± 2 °C) than those reported for supercooled mixtures of the same composition with PEO.[20] In turn, that related to LiBr (6 °C) is intermediate between those of $LiClO_4$ and $LiCF_3SO_3$. These T_g data provide further explanation for the differences in the T_g splitting observed in Figure 4. The small splitting observed for the PPO–$LiCF_3SO_3$ system is mainly due to the low T_g of the 10/1 microphase of this system. This feature, which also applies to the PPO–$LiN(CF_3SO_2)_2$ system, is aggravated by the lower salt content in the 16/1 microphase of this system. In turn, although the T_g elevation produced by LiBr is not as marked as that produced by $LiClO_4$, the T_g splitting related to this salt

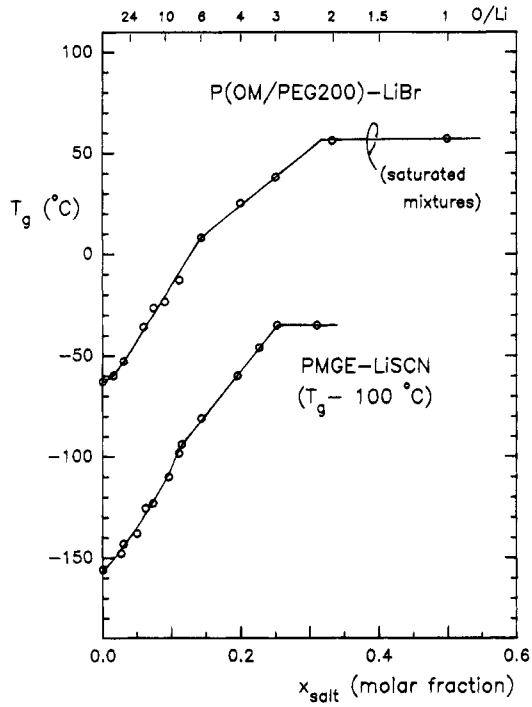

Figure 8. Plots of T_g as a function of the salt molar fraction for amorphous mixtures of the P(OM/PEG200)–LiBr and PMGE–LiSCN systems. No T_g splitting or broadening was observed for these systems.

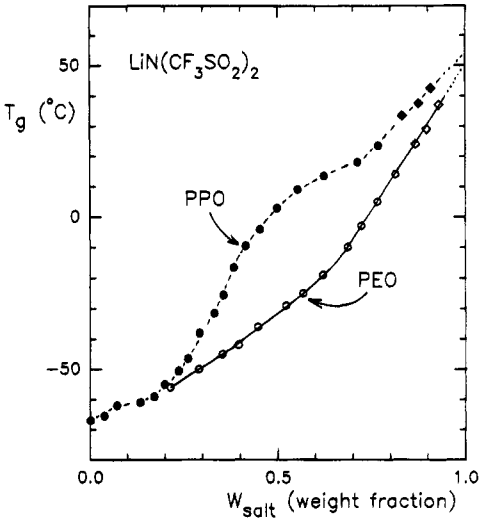

Figure 9. Plots of T_g as a function of the salt weight fraction for mixtures of $LiN(CF_3SO_2)_2$ with PPO and for supercooled mixtures of this salt with PEO. The diamond symbols, which correspond to supersaturated, homogeneous mixtures of either system, allow the definition of the polymer-in-salt regime, i.e., the region where the fully complexed polymer is dissolved in the molten salt.

is enhanced by the larger salt content in its 9/1 microphase.

Figure 8 depicts the T_g–composition relationships constructed for the P(OM/PEG200)–LiBr and PMGE–LiSCN systems. These relationships exhibit the same feature as that of the POP–$LiCF_3SO_3$ system (Figure 6). With increasing salt content, T_g first exhibits an accelerated rise up to a certain composition (O/Li = 6 for $LiCF_3SO_3$, O/Li = 7 for LiBr, and O/Li = 8 for LiSCN) and then increases linearly up to saturation. An initial, accelerated rise is also observed for the PPO–$LiN(CF_3SO_2)_2$ system (Figure 6), but a more gradual change takes place at higher concentrations. Note that supercooled mixtures of PEO with $LiClO_4$, $LiCF_3SO_3$, $LiN(CF_3SO_2)_2$, and LiSCN were reported to exhibit a linear increase in T_g over this range.[19,20] Thus, the data in Figure 8 suggest some kind of microphase separation for the P(OM/PEG200)–LiBr and PMGE–LiSCN systems, even though no T_g splitting or broadening could be detected in the DSC curves of these systems.

According to the ceiling values of T_g in Figures 2 and 6, at moderate temperatures and on a molar basis, the solubility limits of the present salts increase in the order $LiClO_4$ < LiBr < $LiCF_3SO_3$ < $LiN(CF_3SO_2)_2$, that is, in the same order as $T_{g,L}$ in Figure 4. At their melting points, $LiClO_4$ (T_m = 251 °C) and $LiN(CF_3SO_2)_2$ (T_m = 234 °C) are fully miscible with PPO. As could be judged by microscopy, $LiCF_3SO_3$ and LiBr, which melt at much higher temperatures, both exhibit a minute increase in solubility over the range 70–250 °C. As reported for PEO,[5] melt quenching of PPO–$LiN(CF_3SO_2)_2$ mixtures from a temperature above the melting point of the salt yields supersaturated mixtures in the vitreous state. In Figure 9, the T_g data of these mixtures (diamond symbols) are plotted as a function of the salt weight fraction for both polymers. These plots, which include the data of the unsaturated mixtures, show a change of regime at W_{salt} = 0.70 (O/Li = 2) for PPO and near W_{salt} = 0.65 (O/salt = 3.5) for PEO. More concentrated mixtures yield linear relationships that converge toward the same limit (T_g = 52 ± 2 °C) at a 100% salt content. These new relationships suggest that the materials then consist of fully complexed PPO (or PEO) dissolved in the molten salt. Therefore, it is the physical properties of the fully complexed polymer that govern the T_g elevation at lower salt contents.[5] This latter feature should also apply to the other systems.

(b) Conductivity Study. By analogy with microphase-separated block copolymers, the low-T_g microphase in the present PPO–LiX electrolytes should transform into a continuous phase below a certain salt content. If this hypothesis is correct, this change should strongly affect the conductivity behavior. This is particularly true for the PPO–$LiClO_4$ system, which exhibits the lowest values of $T_{g,L}$ among the present systems. On the other hand, if such an effect exists, it will be less severe for the PPO–$LiN(CF_3SO_2)_2$ system, which exhibits the highest values of $T_{g,L}$ among the present systems. In order to clarify this point, we chose a comparison with the corresponding PEO–LiX systems. As reported in a previous work,[20] the conductivity isotherms of these two PEO systems show broad maxima of comparable magnitude over the range where a T_g splitting (or broadening) is observed in PPO. Also, their phase diagrams, together with the supercooling of certain compositions, allow a conductivity study down to 50 °C over a wide range of compositions.[5,20]

In Figure 10, conductivity data (σ) obtained for the PEO–$LiClO_4$ system are compared with the data reported by McLin and Angell[8] for a PPO sample of the same molecular weight ($M = 4 \times 10^3$) as the PEO and PPO samples used in this study. These conductivity isotherms (at 50 °C), showing log σ as a function of the salt molar fraction, do not reveal any anomaly that could be associated with microphase separation. This also applies to the PEO– and PPO–$LiN(CF_3SO_2)_2$ systems, whose conductivity isotherms (at 100 °C) are included in Figure 10. The data obtained for the latter system cover the same range of compositions as those recently reported for the PEO–$LiN(CF_3SO_2)_2$ system.[5]

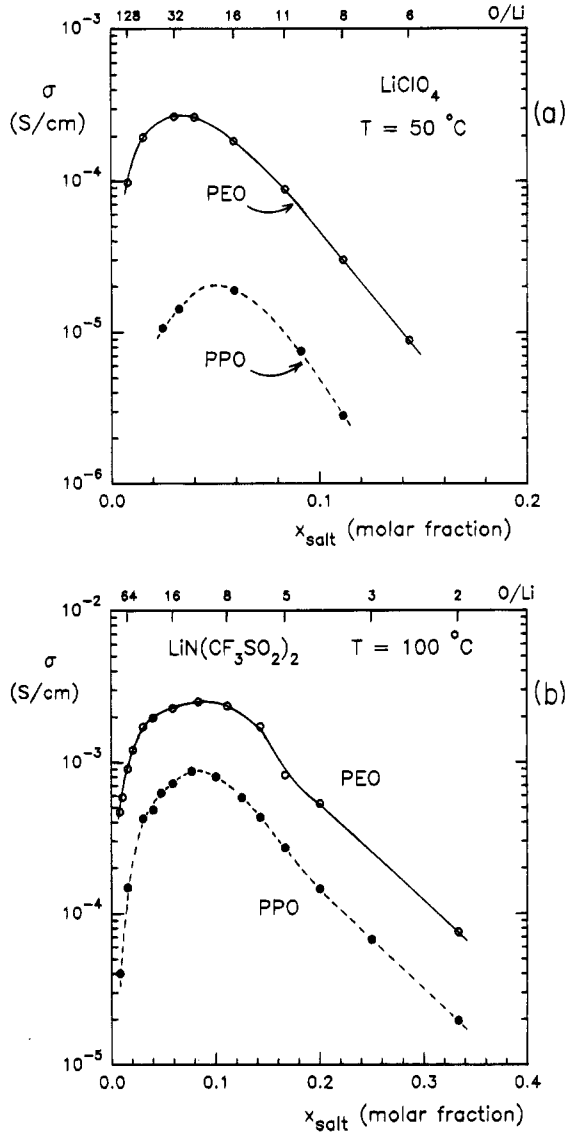

Figure 10. Conductivity isotherms of the PPO–$LiClO_4$ system at 50 °C (a) and the PPO–$LiN(CF_3SO_2)_2$ system at 100 °C (b). In each case, a comparison is made with amorphous electrolytes of the same salt in PEO. The data of the PPO–$LiClO_4$ system are those reported by McLin and Angell.[8]

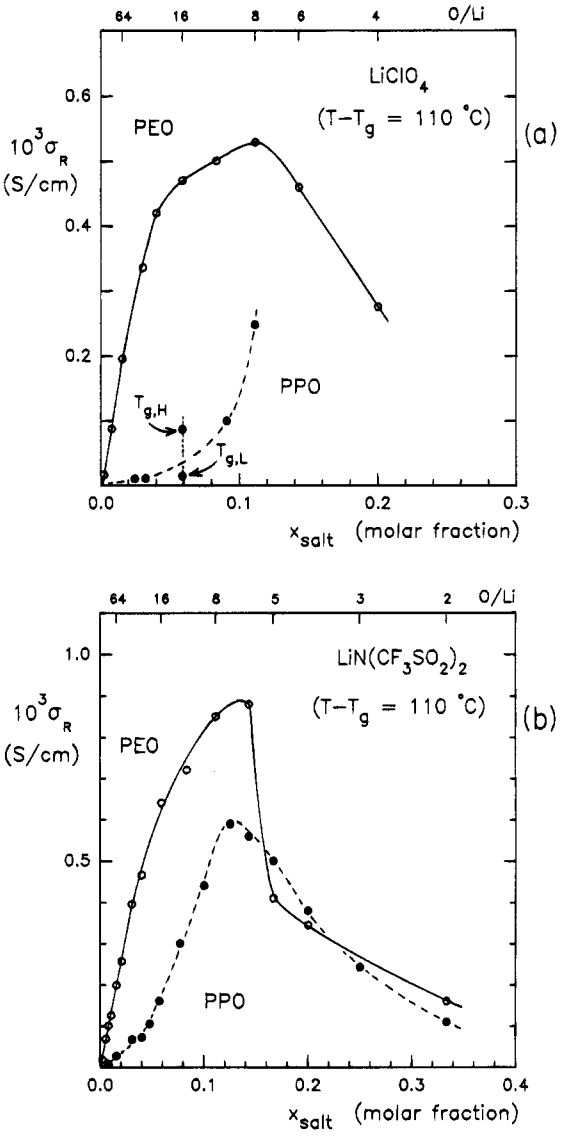

Figure 11. Reduced conductivity at $T - T_g = 110$ °C of the PPO–$LiClO_4$ (a) and PPO–$LiN(CF_3SO_2)_2$ (b) systems. A comparison with related PEO amorphous electrolytes shows evidence for a percolation threshold near the critical composition for microphase separation in PPO.

The broad maxima in Figure 10 result from a change in charge carrier mobility with increasing salt concentration. Since local viscosity accounts for a large part of this effect, further analysis of the present data will be made in terms of reduced conductivity σ_R, i.e., conductivity at a given value of $T - T_g$. A reduced temperature $T - T_g$ of 110 °C was chosen for that purpose. It is within the narrow range of $T - T_g$ that allows a comparison with the σ_R data of the PEO electrolytes.[23] In the case of the PPO–$LiClO_4$ and PPO–$LiN(CF_3SO_2)_2$ systems, the actual temperatures were established on the basis of the T_g data of Figures 2 and 6. For the latter system, which was studied over the range $2 \leq$ O/Li < 128, these temperatures extend from 45 to 130 °C, approximately. Two of the studied compositions (O/Li = 20 and 24) are within the range where a T_g broadening is observed in Figure 1. No attempts were made to consider this broadening (the onset of the main transition was used for all compositions). For the PPO–$LiClO_4$ system, however, both the values of $T_{g,L}$ and $T_{g,H}$ were considered, yet such a T_g splitting applies to a single composition only (O/Li = 16). Such a blind procedure was used on purpose. The aim of this comparison is to look for any anomaly with respect to PEO that could be attributed to microphase separation in PPO.

Figure 11 shows plots of σ_R as a function of the molar fraction of $LiClO_4$ and $LiN(CF_3SO_2)_2$ in PPO and PEO. These nonlogarithmic plots made under isoviscous conditions reveal that microphase separation has a marked effect on the conduction process. For the PPO–$LiClO_4$ system, σ_R first increases very slowly with increasing concentration up to the composition O/Li = 10 and then exhibits an accelerated rise toward σ_R of the PEO–$LiClO_4$ system. Over the same range, the PEO systems first exhibit a linear increase in σ_R followed by a decrease above a certain salt content. A similar difference between PPO and PEO is observed in systems containing the second salt. However, the initial rise in σ_R for the PPO–$LiN(CF_3SO_2)_2$ system is not as flat as in the case of the PPO–$LiClO_4$ system.

It may be seen that the value of σ_R established on the basis of $T_{g,H}$ (−35 °C) for the PPO–$LiClO_4$ mixture in a ratio O/Li = 16 is well above the curve drawn through the data of the other compositions. In turn, that

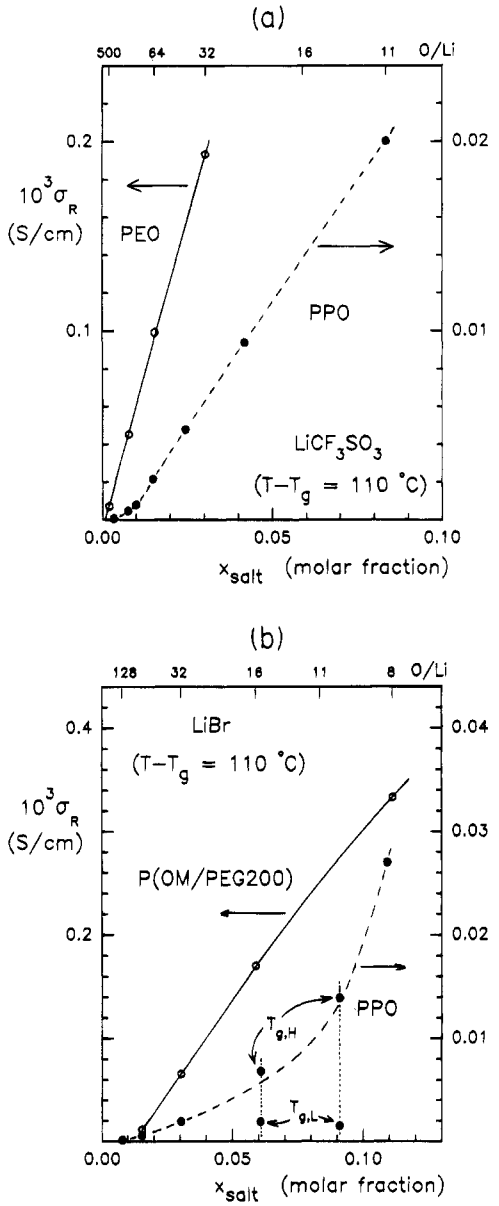

Figure 12. Reduced conductivity at $T - T_g = 110$ °C of the PPO–$LiCF_3SO_3$ (a) and PPO–LiBr (b) systems. The σ_R data of the former system are based on a work by Albinsson *et al.*[9] A comparison with PEO or P(OM/PEG200) amorphous electrolytes shows the same features as in Figure 11.

established on the basis of $T_{g,L}$ (−64 °C) is below but closer to this curve. In fact, a good fit can be made by adjusting T_g to −58 °C, i.e., 11 °C only above the T_g of salt-free PPO. In comparison, the T_g of a PEO–$LiClO_4$ supercooled mixture of the same composition is −43 °C. From this departure, it is clear that the conduction process is severely affected by the presence of the low-T_g microphase. According to the Δc_p data in Figure 3, such a mixture with a molar ratio O/Li = 16 (W_{salt} = 0.10) should contain 63% by weight of the high-T_g microphase. As reported by Wixwat *et al.*,[24] over the temperature range from 33 to 90 °C, the density of a PPO–$LiClO_4$ mixture with a molar ratio O/Li = 10 (the composition of the high-T_g microphase) is 12% higher than that of salt-free PPO. By assuming that this difference in density applies to the unlike microphases in the O/Li = 16 mixture, the volume fraction of its high-T_g microphase may be estimated as 56%. This volume fraction is high enough to suggest that the accelerated rise in σ_R observed at higher salt contents corresponds to a percolation threshold. As will be shown, this feature, which takes place just above the range where a T_g splitting (or broadening) is observed in the DSC curves, is a general feature of the PPO–LiX electrolytes in this study.

Two other interesting features can be deduced from the σ_R plots in Figure 11. The first concerns the composition of the low-T_g microphase in the mixtures of the PPO–$LiClO_4$ system. The finite value of σ_R (1.04 × 10^{-5} S/cm) at the lower end of the concentration range of this system (O/Li = 40) indicates that this microphase contains a certain amount of salt. However, this amount is relatively small since this value of σ_R is inferior to that (1.65 × 10^{-5} S/cm) of the PEO–$LiClO_4$ mixture with a molar ratio O/Li = 500. The second feature concerns the superposition of the PPO– and PEO–$LiN(CF_3SO_2)_2$ data above a certain concentration in the concentrated regime. The abrupt decrease in σ_R over this range is the prelude to the changes of regime observed at high concentrations in the T_g plots of Figure 9. Less and less free ether units are available for cation jumps, and a second percolation threshold takes place in both polymers this time.[5]

As mentioned, amorphous electrolytes cannot be obtained at moderate temperatures for the PEO–LiBr system. A similar but less severe limitation also applies to the PEO–$LiCF_3SO_3$ system. Although its phase diagram also involves a high-temperature liquidus curve at low salt contents,[20] by taking advantage of the greater salt content in the eutectic mixture of this system (O/Li = 40), conductivity data could be obtained over the range 32 < O/Li < 500. These data, as well as those reported by Albinsson *et al.*[9] for a $M = 4 \times 10^3$ PPO sample, allowed the construction of the σ_R plots described in Figure 12. These plots show the same features as those related to $LiN(CF_3SO_2)_2$ in Figure 11. Note that none of the PPO–$LiCF_3SO_3$ mixtures are located over the range (14 < O/Li < 20) where a T_g splitting is observed in Figure 1. Included in Figure 12 is a second comparison based on conductivity data obtained for the PPO–LiBr and P(OM/PEG200)–LiBr systems. It may be seen that the former system behaves like the PPO–$LiClO_4$ system. Furthermore, in agreement with the expectation based on the singularity observed in the T_g plot of the P(OM/PEG200)–LiBr system (Figure 8), its σ_R plot also exhibits an accelerated rise at low salt contents.

As illustrated in Figure 13, σ_R plots constructed from conductivity data obtained for the PMGE–LiSCN and PEO–LiSCN systems also show that a similar anomaly exists in PMGE. This latter comparison is particularly interesting since LiSCN is among the lithium salts that exhibit the lowest conductivities in PEO. For the composition O/Li = 32, its value of σ_R is 0.6 × 10^{-4} S/cm compared to 4.0 × 10^{-4} S/cm for $LiN(CF_3SO_2)_2$. By assuming that this difference is mainly due to a greater association of LiSCN in PEO, it is noticeable that this latter system yields a linear rise in σ_R at low concentrations similar to that of the PEO–$LiN(CF_3SO_2)_2$ system. Therefore, the accelerated, nonlinear rises observed in POP and PMGE cannot be attributed to ion pairing.

Concluding Remarks

Two distinct effects account for the low conductivity of PPO–LiX electrolytes with respect to related PEO–LiX amorphous electrolytes. One of these effects, which mainly concerns the concentrated regime (O/Li < 10),

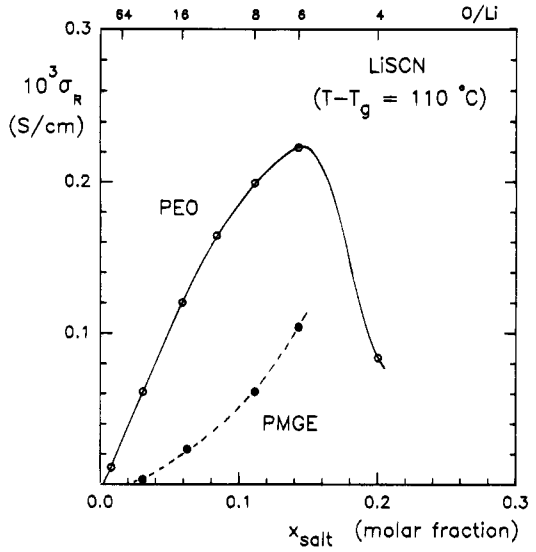

Figure 13. Reduced conductivity at $T - T_g = 110$ °C of the PMGE–LiSCN system. A comparison with PEO–LiSCN amorphous electrolytes shows the same features as those of the PPO–LiX systems in Figures 11 and 12.

is the greater T_g elevations produced by the presence of the salts in the former electrolytes. The second effect, which concerns both the semidilute and the dilute regimes, is microphase separation. This phenomenon, which is not unique to PPO, causes a marked depression in conductivity over the range where related PEO electrolytes exhibit their conductivity maximum. When combined, these two effects result in a global lowering of the conductivity isotherms over the entire range of compositions. As shown in this work, when the former of these effects is separated from the latter in terms of reduced, isoviscous conductivity, a signature specific to microphase separation clearly appears into the concentration dependence of the data. This signature is an initial low conductivity regime followed by an abrupt rise near the critical composition for microphase separation. For the PPO–$LiClO_4$ and PPO–LiBr systems, which involve a large difference between the compositions of their unlike microphases, this feature is clear evidence for a percolation threshold.

Interestingly, non-PPO systems, like the PMGE–LiSCN and P(OM/PEG200)–LiBr systems, also show anomalies that may be interpreted in terms of microphase separation. Over a range of compositions, both their T_g and their reduced conductivity exhibit accelerated rises similar to those of the PPO–$LiCF_3SO_3$ and PPO–$LiN(CF_3SO_2)_2$ systems. The absence of any T_g splitting or broadening, however, suggests the presence of more labile heterogeneities than in these latter systems. Note that all the PEO–LiX systems studied until now appear to be free from such anomalies. However, at the present time, it is not clear whether the results obtained for the P(OM/PEG200)–LiBr system depend on the nature of the salt or the nature of the polymer (or both). This segmented copolymer contains 80% of EO units, and it is noticeable that microphase separation still takes place in a propylene oxide–ethylene oxide statistical copolymer containing 90% of EO units.[18] This confirms that regular PEO is unique among the polyethers and copolyethers that can dissolve metal salts.

A last point concerns the effect of temperature and pressure on the compositional features of microphase-separated PPO electrolytes. Raman data reported by Schantz[6] show that an increase in temperature in the dilute regime (100 < O/salt < 1000) has the same effect as an increase in concentration at a given temperature in the concentrated regime (5 < O/salt < 10). For instance, at 67 °C the two components associated with the anion symmetric stretching mode in PPO–$LiClO_4$ dilute electrolytes exhibit the same relative intensities as those expected for the composition O/Li = 7 at 22 °C. More recent data reported by Lundin and Jacobsson[12] show that an increase in pressure gives rise to the opposite effect in Raman spectra recorded on PPO–$LiCF_3SO_3$ electrolytes with molar ratios O/Li = 16 and 32. Both these effects were discussed in terms of a change in ion pairing with increasing temperature (or pressure) without any concern about the possibility for a microphase separation.

Since a large fraction of the salt (particularly $LiClO_4$) is confined to the high-T_g microphase of these systems, a new interpretation of the Raman data should focus on a potential change in the composition of this microphase. Note that Raman spectra recorded at a given temperature, under normal pressure, show no apparent changes resulting from the decrease in the size of the concentrated microdomains with dilution.[6,10,11] These microdomains form spontaneously because their stoichiometry involves a maximum of interactions with a minimum of internal tension. The ion–ion long-range Coulombic energy, which is dominant in the stabilization of this structure, strongly depends on the average distance between the ions. Therefore, it is likely that, in order to minimize the free energy, the stoichiometry of these microdomains readjusts to either a lower or a larger salt content in response to compression or thermal expansion. If that is the case, the critical compositions deduced from the T_g data would correspond to low-temperature conditions. The possibility that these critical compositions may shift to higher salt contents with increasing temperature does not change the main features deduced from the present data.

Acknowledgment. This work was supported by the Research Institute of Hydro-Quebec (IREQ) and the Natural Sciences and Engineering Research Council of Canada.

References and Notes

(1) Armand, M. *Solid State Ionics* **1994**, *69*, 309.
(2) Gray, F. M. *Solid Polymer Electrolytes*; VCH Publishers: New York, 1991.
(3) Barthel, J.; Gores, H. J.; Schmeer, G.; Watchter, R. In *Topics in Current Chemistry*; Boschke, F. L., Ed.; Springer-Verlag: New York, 1983; Vol. 111, p 33.
(4) Besner, S.; Vallée, A.; Bouchard, G.; Prud'homme, J. *Macromolecules* **1992**, *25*, 6480.
(5) Lascaud, S.; Perrier, M.; Vallée, A.; Besner, S.; Prud'homme, J.; Armand, M. *Macromolecules* **1994**, *27*, 7469.
(6) Schantz, S. *J. Chem. Phys.* **1991**, *94*, 6296.
(7) Schantz, S.; Torell, L. M. *Solid State Ionics* **1993**, *60*, 47.
(8) McLin, M. G.; Angell, C. A. *J. Phys. Chem.* **1991**, *95*, 9464.
(9) Albinsson, I.; Mellander, B.-E.; Stevens, J. R. *J. Chem. Phys.* **1992**, *96*, 681.
(10) Manning, J.; Frech, R. *Polymer* **1992**, *33*, 3487.
(11) Bernson, A.; Lindgren, J. *Solid State Ionics* **1993**, *60*, 37.
(12) Lundin, A.; Jacobsson, P. *Solid State Ionics* **1993**, *60*, 43.
(13) Fishburn, J. R.; Barton, S. W. *Macromolecules* **1995**, *28*, 1903.
(14) Vachon, C.; Vasco, M.; Perrier, M.; Prud'homme, J. *Macromolecules* **1993**, *26*, 4023.
(15) Bergman, R.; Börjesson, L.; Fytas, G.; Torell, L. M. *J. Non-Cryst. Solids* **1994**, *172–174*, 830.
(16) Moacanin, J.; Cuddihy, E. F. *J. Polym. Sci., Part C* **1966**, *14*, 313.

(17) Greenbaum, S. G.; Pak, Y. S.; Wintersgill, M. C.; Fontanella, J. J. *Solid State Ionics* **1988**, *31*, 241.
(18) Nekoomanesh, H. M.; Wilson, D. J.; Booth, C.; Owen, J. R. *J. Mater. Chem.* **1994**, *4*, 1785.
(19) Dumont, M.; Boils, D.; Harvey, P. E.; Prud'homme, J. *Macromolecules* **1991**, *24*, 1791.
(20) Vallée, A.; Besner, S.; Prud'homme, J. *Electrochim. Acta* **1992**, *37*, 1579.
(21) Booth, C.; Nicholas, C. V.; Wilson, D. J. In *Polymer Electrolyte Reviews*; MacCallum, J. R., Vincent, C. A., Eds.; Elsevier Applied Sciences: New York, 1989; Vol. 2, p 229.
(22) Denault, J.; Morèse-Séguéla, B.; Séguéla, R.; Prud'homme, J. *Macromolecules* **1990**, *23*, 4658.
(23) Most of the PEO–LiX systems were studied down to high dilution (O/Li = 500). Since mixtures with O/Li ⩾ 32 could not be supercooled by melt quenching, their T_g data were obtained by linear extrapolation on plots of T_g as a function of the salt molar fraction. Also, for mixtures with O/Li ⩾ 64, the temperatures corresponding to $T - T_g - 110$ °C were a few degrees below the limit of 50 °C imposed by crystallization. Their σ_R data were obtained by linear extrapolation on plots of ln σ as a function of $(T - T_g + 25)^{-1}$.
(24) Wixwat, W.; Fu, Y.; Stevens, J. R. *Polymer* **1991**, *32*, 1181.

MA9504835